

**PART III:**

# FGS

---

**Chapter 9: FGS Instrument Overview**

**Chapter 10: FGS Data Structures**

**Chapter 11: FGS Calibration**

**Chapter 12: FGS Error Sources**

**Chapter 13: FGS Data Analysis**

■ FGS

# FGS Overview

### In This Chapter...

FGS Capabilities / 9-2
FGS Design / 9-3
FGS Control / 9-15
Target Acquisition and Tracking / 9-16
Transfer Scans / 9-21
FGS Guiding / 9-21
FGS Astrometry / 9-22
Astrometry with FGS 3 / 9-23

The primary purpose of the three Fine Guidance Sensors (FGS) on HST is to maintain the pointing stability of the telescope at the milliarcsecond level. The FGSs, designed and built by Hughes Danbury Optical Systems (HDOS), routinely point the spacecraft with a precision of 5 mas or less. As part of the second servicing mission, HDOS upgraded the spare FGS, which replaced the original in Bay #1, with a commandable mechanism to enhance the instrument's performance. HDOS is currently upgrading the returned FGS1 for an expected return to the telescope during the third servicing mission.

The high precision of the FGSs makes them excellent astrometers. The narrow point spread function of HST and the dynamic range of the FGS make it an unparalleled science instrument for many important astronomical investigations. Detecting and resolving multiple star systems and planetary companions, delineation of objects in crowded fields, measuring stellar angular diameters, parallax, proper motion, positional surveys, occultation studies and photometry are among its many uses. This chapter describes how each Fine Guidance Sensor operates, summarizing its capabilities, its design, and its modes of operation.

## 9.1 FGS Capabilities

Each Fine Guidance Sensor on HST is an optical-mechanical white-light interferometer that can sense 1–2 milliarcsecond (mas) angular displacements of a point source in two dimensions over the range of apparent visual magnitudes from  $3 < V < 15$ . It can observe fainter objects down to  $V < 17$ , but its accuracy degrades to more than 2 mas. The instrument's spectral response is fairly flat from 4000 Å to 7200 Å, although more sensitive in the red, with sharp drop-offs outside this range.

The optical path through an FGS is complex because the beam passes through multiple optical elements. The relative alignment of all these components and the wavelength dependencies introduced by their reflective surfaces and refractive optics impose the resolution and magnitude limits of the FGS. Most of the FGS calibration procedure consists of empirical and semi-empirical subtraction of the instrument's signature, necessitating observations of standard stars in various spectral ranges and all modes of observation.

The three FGSs on board HST occupy three of the four radial bays. Normally two FGSs are used for pitch, yaw, and roll control of the telescope, leaving one available for astrometry. The telemetry from the guiding FGSs is captured and processed by the ground system and stored in the Hubble Data Archive. The processed FGS data can be retrieved for any HST observation in the form of OMS files (see Appendix B), which provide information on spacecraft jitter. However, the data files associated with an FGS astrometry observation, which are used in the FGS calibration pipeline, record jitter information at a much higher time resolution (40 Hz as compared to 0.33 Hz).

An FGS can be used for astrometry in two different modes:

- POSITION mode, in which it tracks an object, measuring its precise location.
- TRANSFER mode, in which it scans across an object, such as a binary star system, resolving its structure.

POSITION mode observing is used both to guide the telescope and for positional astrometry. TRANSFER mode is used primarily to support astrometry science programs investigating multiple star systems or extended objects, but is on occasion used in engineering tests to evaluate the FGS and the OTA optical systems.

FGS 3 is currently designated and calibrated as an astrometer. This FGS can measure point-source angular positions of 1–2 mas over the brightness range of 3 to 17 magnitudes and can resolve the components of binary systems with separations as small as 15 mas. For many scientific studies, this FGS continues to exceed ground based efforts in sensitivity, dynamic range, and resolution.

## 9.2 FGS Design

This section describes the Fine Guidance Sensor design, its optical train, the aperture, the S-curves that give the response of the instrument to positional changes, and the enhancements made to the refurbished FGS 1R, installed during the February 1997 servicing mission.

### 9.2.1 FGS Optics

An FGS is essentially a pair of two orthogonal white-light, equal-path interferometers, their associated optical and mechanical elements, and four photo-multiplier tubes (PMTs). Light from an object is collected by the telescope's primary mirror, reflected and focused by the secondary mirror, intercepted by a plane pickoff mirror before the focal point, and directed into the FGS and onto the Aspheric Collimating Mirror to produce a nearly collimated beam. The ray is directed to the optical elements of the Star Selector A (SSA) assembly. This rigid assembly of two mirrors and a five element corrector group can be commanded to rotate about HST's optical axis (V1). Two mirrors in the Star Selector A assembly deflect the beam and direct it through the five element corrector group that performs the final collimation and corrects for the optical aberrations induced by the aspheric mirror. They do not correct the spherical aberration arising from HST's mis-figured primary mirror.

The direction of the exit ray depends upon the incoming beam's angle of incidence on the SSA assembly, and therefore the rotation position of SSA and the beam's point of origin on the aspheric mirror which is, in turn, determined by the angle between the spacecraft's optical axis (V1) and the position of the star on the sky.

After exiting the SSA assembly the ray encounters a field stop to minimize scattered light and to narrow the field of view. The four mirrors of the Star Selector B (SSB) assembly receive the ray and redirect it through the filter wheel assembly and a plane fold flat mirror (FF3) reflects it onto the polarizing beam splitter. Like the SSA assembly, the SSB assembly can be commanded to rotate within HST's focal plane. Together the SSA and SSB assemblies transmit to the polarizing beam splitter only those photons originating from a narrowly defined direction, masking out all but a small (5" x 5") area of sky.

The polarizing beam splitter divides the incoming unpolarized light into two linearly plane polarized beams with orthogonal polarizations, each having roughly half the incident intensity, and directs them to the two Koesters prisms and their associated optics, field stops, and photomultiplier tubes (see Figure 9.1). Each of the two output rays from the polarizing beam splitter fall upon the face of the appropriate Koesters prism.

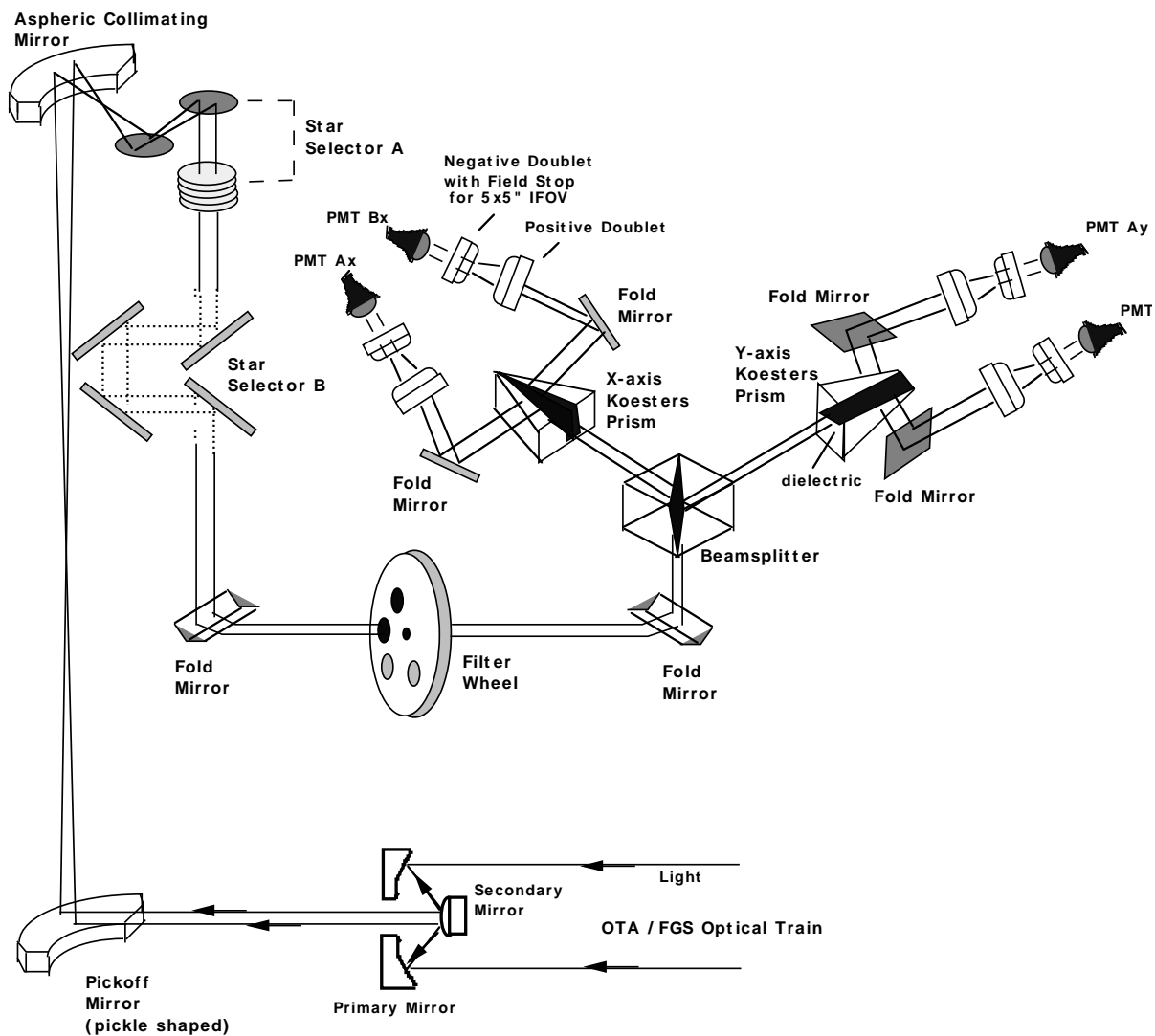
The Koesters prisms are constructed of two halves of fused silica joined together along a surface coated to act as a dielectric beam splitter. The dielectric performs an equal intensity division, introducing a 90 degree phase difference between the reflected and transmitted portions of the beam, with the transmitted

lagging the reflected. This division gives the Koesters prism its interferometric properties because the beam reflected from one side of the prism, when joined with the transmitted beam from the other side, constructively or destructively interferes to a degree depending upon the angle between the incoming wavefront and the entrance face. Each Koesters prism thus emits two collimated exit beams whose relative intensities depend upon the tilt of the incident wavefront. Each beam is then focused and passed through a field stop to illuminate the surface of a photomultiplier tube (PMT) which records the number of photons received during each 25 msec interval.

The collimated beam entering each Koesters prism can be characterized by a propagation vector. The Koesters prism senses the tilt of this incident wavefront only in the direction perpendicular to the plane of the dielectric surface. Small rotations of the star selector A and B assemblies can change the direction of the propagation vector, and hence the tilt of the incident wavefront at the face of the Koesters prism. When the component of the wavefront's propagation vector perpendicular to the plane of the dielectric surface is zero, a condition of interferometric null results, and the relative intensities of the two emergent beams, measured by the PMTs, will ideally be equal. Meanwhile, the other Koesters prism is sensitive to the wavefront's tilt in the orthogonal plane.

Figure 9.1 schematically displays the important optical and mechanical components of an FGS. Each Koesters prism is sensitive to the tilt of the wavefront about an axis which is parallel to the face of the prism and in the plane of the dielectric beam splitter (the shaded area within each prism).

Figure 9.1: The FGS Optical Train



The fine sensitivity of the Koesters prisms to the angle of the incident radiation is what enables the FGS to measure star positions so accurately. For a star at a given position in FGS's detector space, there is a unique rotational position for each of the star selector A,B assemblies which brings that star's wavefront to zero tilt at the face of each Koesters prism. Therefore, the position of the star in the FGS detector space, and equivalently in HST's focal plane, can be measured precisely and accurately. Ultimately, the reliability of such measurements depends on the calibration of the instrument.

An  $(x,y)$  coordinate system maps the detector space of an FGS. The Koesters prisms are aligned such that one is sensitive to angular displacements along the  $x$  direction, the other along the  $y$  direction. Because each Koesters prism has two associated PMTs, each FGS has four PMTs in all. The two PMTs associated with

the  $x$ -axis Koesters prism are labeled PMTXA and PMTXB. The other pair, associated with the  $y$ -axis Koesters prism, are labeled PMTYA and PMTYB.




---

Note that the FGS  $(x,y)$  detector coordinate system differs from the POS TARG coordinate system in the Phase II proposal instructions. The FGS coordinates originate from the telescope's optical axis (V1 bore sight) while the POS TARG system originates from the center of the detector's field of view. The POS TARG system is used to conveniently define offsets.

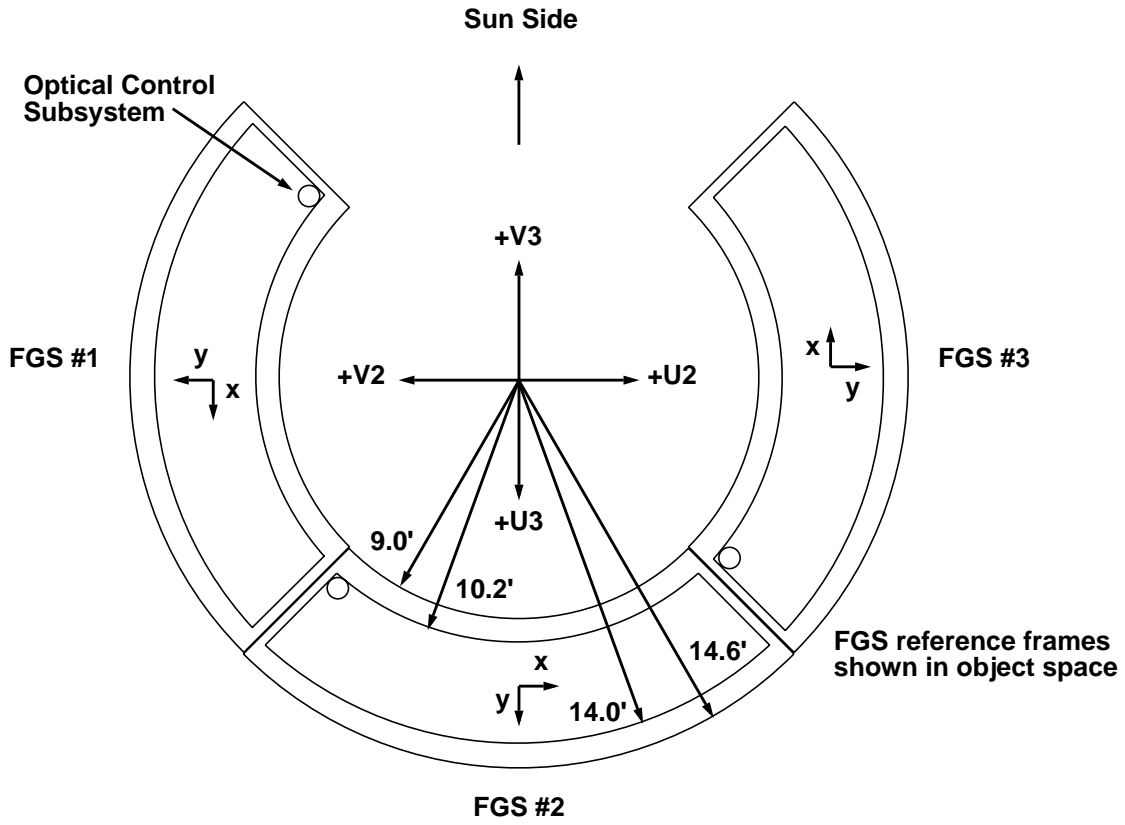
---

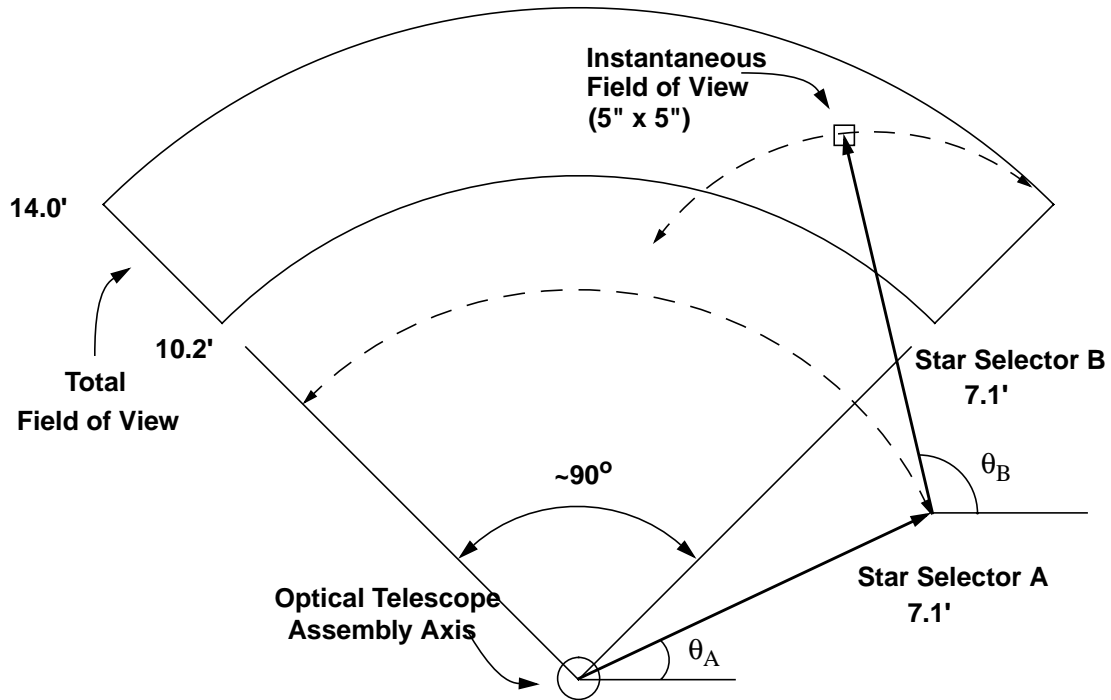
### 9.2.2 FGS Aperture

The instrument's total field of view (FOV), referred to as a *pickle* because it vaguely resembles the shape of a pickle, is a quarter annulus in the HST's focal plane, extending radially 10' to 14' from the telescope's boresight and axially 83.3° on the inner arc and 85° on its outer arc, an area of approximately 69 square arcminutes. The instantaneous field of view (IFOV) determined by the star selector assemblies and field stops is far smaller—5" by 5"—and its location within the pickle depends upon the Star Selector A and B rotation angles. Only those photons entering this IFOV aperture will be registered by the PMTs. To observe stars elsewhere, the star selector assemblies must be rotated to bring the IFOV to the target. This procedure is called *slewing* the IFOV.

The  $(x,y)$  location of the IFOV in the total FOV is determined from the rotation angles of the star selector A,B assemblies. Each FGS has its own detector space  $(x,y)$  coordinate system which maps into HST's (V1,V2,V3) coordinate system. FGS 2, and FGS 3 are nominally oriented at 90, and 180 degrees with respect to FGS 1, but small angular deviations are present. The FGS-to-FGS alignment matrix in the onboard flight software accounts for these deviations. Figure 9.2 and Figure 9.3 show the FGSs and their coordinate systems in the HST focal plane.

**Figure 9.2:** FGS Field of View (pickle) the HST Focal Plane with Local (x,y) Coordinate System Related to HST (V2,V3) System.

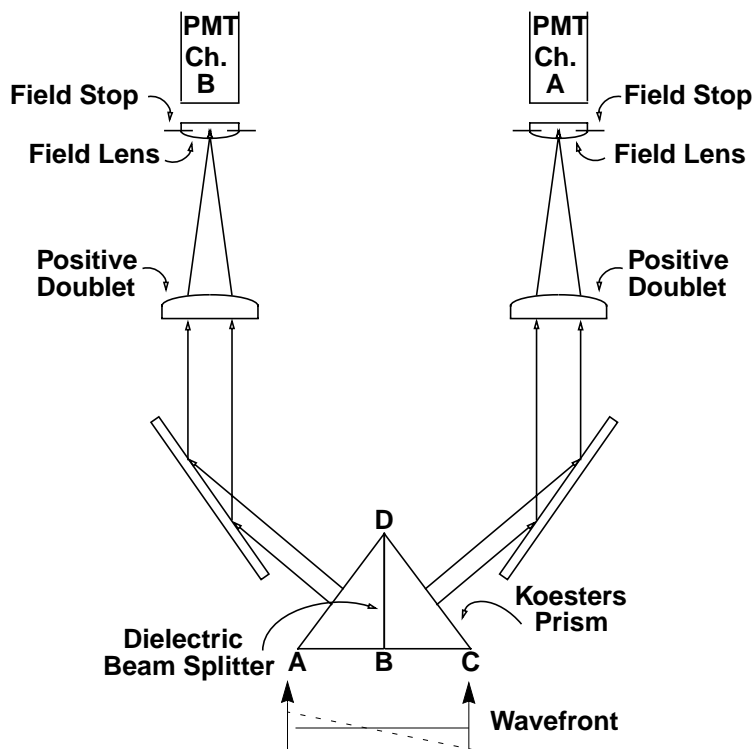


**Figure 9.3:** IFOV Placement in Pickle by Rotating SSA and SSB.

### 9.2.3 S-curves

As discussed earlier, each Koesters prism in an FGS is sensitive to the tilt of the incident wavefront in the direction perpendicular to the dielectric surface joining the two halves of the prism (see Figure 9.4, and Figure 9.5). Assuming the presence of a luminous point source in the IFOV, the relative intensity of the beams emerging from each Koesters prism is determined by the wavefront's tilt, and therefore responds to the rotations of the SSA and SSB assemblies that scan the IFOV across the star. The responses of the PMTs during such a scan provide the characteristic interferometric signature of the FGS. Graphing the normalized difference of the PMTs corresponding to a given channel against the position of the IFOV in detector space produces a figure known as an *S-curve*.

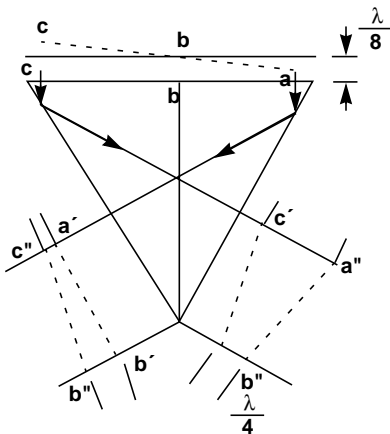
**Figure 9.4:** Emergent Beams from Koesters Prism and Photo-multiplier Tubes. The Koesters prism is sensitive to the tilt of the wavefront about an axis normal to the page and intersecting point B.



FGS/9

Figure 9.5 shows how a Koesters prism generates the characteristic S-curves shown in Figure 9.6. As the wavefront rotates about point B, the relative intensities of the two emergent beams change as a function of the tilt angle. If the tilt axis is not at point B, the beam is said to be *decentered* and the S-curve's morphology and modulation are degraded. Unfortunately, because HST's wavefront is spherically aberrated, a small decenter of the beam (0.5%) will cause 25% degradation of the S-curve's signal.

**Figure 9.5:** Internal Reflection and Transmission of the Beam Entering the Koesters Prism on the AC Face

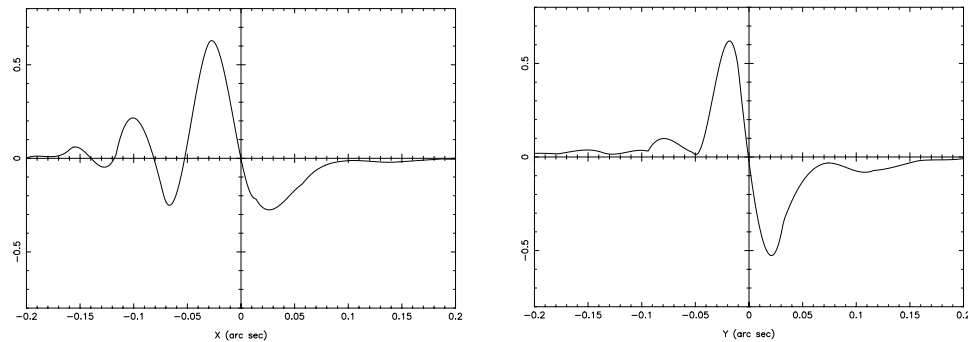


The Koesters prisms measure the two orthogonal wavefront directions and thus produces two S-curves,  $S_x$  and  $S_y$ . The  $x$ -axis S-curve is given by:

$$S_x = (A_x - B_x) / (A_x + B_x)$$

where  $A_x$  is the photon count from PMTXA (accumulated over 25msec), and  $B_x$  is the count from PMTXB. The  $y$ -axis S-curve is computed in a similar way. Figure 9.6 shows the S-curves for the  $x$  and  $y$  axes observed near the center of the field of view of FGS 3. When the IFOV is more than 100 mas from the location of interferometric null, the PMTs of a given channel record nearly equal intensities. But closer to the interferometric null a signal emerges as the Koesters prism produces beams of different relative intensities. The so-called *zero point crossing* between the  $+/-$  peaks of the S-curve ideally occurs at interferometric null. Note however, that the relative sensitivities of the PMTs and the optical paths traversed by the beam after emerging from the Koesters prism are not identical, and therefore, the zero point crossing may not occur exactly at the interferometric null. (This effect is accounted for in the data reduction process.) Because a one-to-one relationship exists between the rotation angles of the Star Selector A and Star Selector B assemblies and the  $x,y$  detector space coordinates, the values of these rotation angles at interferometric null can be used to measure the position of the star in  $x,y$  detector space.

**Figure 9.6:** FGS 3 S-Curves of Upgren69 in F583W at  $(x,y) = (0,0)$



### Field Dependencies of S-curves

S-curves can be measured anywhere in the FGS FOV. A standard star (UPGREN69) has been observed at nine standard positions within each of the three FGSs. The S-curves obtained from a given FGS are compared among themselves; any variation of the S-curve morphology (its shape) and modulation (its peak to peak amplitude) with position in the pickle is referred to as *field dependency* of the S-curve.

An FGS will display degraded S-curve performance when the collimated beam is not well centered on the face of the Koesters prism. In addition, given the presence of spherical aberration due to the misfigured primary mirror, the wavefront presented to the Koesters prism is not flat but has curvature, a fact that greatly amplifies the effects of optical misalignments. Specifically, a decentered beam in the presence of spherical aberration gives rise to coma and astigmatic aberrations, resulting in degraded S-curve characteristics.

The source of the field dependency is thought to be *beam walk* originating from a misalignment of the star selector B assembly with respect to the Koesters prism that changes as a function of SSB rotation angle. The Star Selectors center the beam on the face of the Koesters prisms while varying the tilt of the wavefront. If there is a clocking error in the alignment of SSB and the Koesters prism, the beam will not remain centered as SSB rotates, resulting in field dependency. Furthermore, if the amount of decentering changes with time, its effects must be monitored in order to calibrate the science data properly. The S-curve measurements in the original three FGSs indicated large decenters of the Koesters prisms in FGS 1 and FGS 2 and strong field dependency in FGS 3.

Figure 9.7 shows that the S-curves of FGS 1 and FGS 2 are not adequate for astrometric science. Only FGS 3 has S-curves with signal-to-noise ratios sufficient for precise astrometry.




---

The face of the Koesters prism is 50 mm wide. In the presence of spherical aberration from the telescope's primary mirror, a decentering of the wavefront by only 0.25mm will decrease the modulation of the S-curve to 75% of its perfectly aligned value. It has been determined that the decenters in FGS 3 range across the pickle from +0.8 to -0.68 (mm) in  $x$  and +0.31 to -0.28 (mm) in  $y$ . If the telescope were not spherically aberrated, mis-alignments up to 5 times this size would not be noticeable.

---

One way to minimize the effects of misalignment and the spherical aberration is to stop down the outer radius of the primary mirror of HST. All the FGSs have a 2/3 pupil stop on their filter wheels. This pupil stop retores the S-curves to a level which allows guiding across the entire pickle. Unfortunately, it also blocks 50% of the target's photons, so nearly a magnitude of sensitivity is lost. Figure 9.8 shows the improvement of the S-curve signature with the 2/3 pupil in place relative to the full aperture for the 3 FGSs at pickle center. Note also the performance of FGS 3 relative to FGS 1 and FGS 2 with full aperture.

**Figure 9.7:** Full-Aperture X and Y Axis S-curves of Original Three FGSs Measured at the Center of Each FGS Field of View

FGS/9

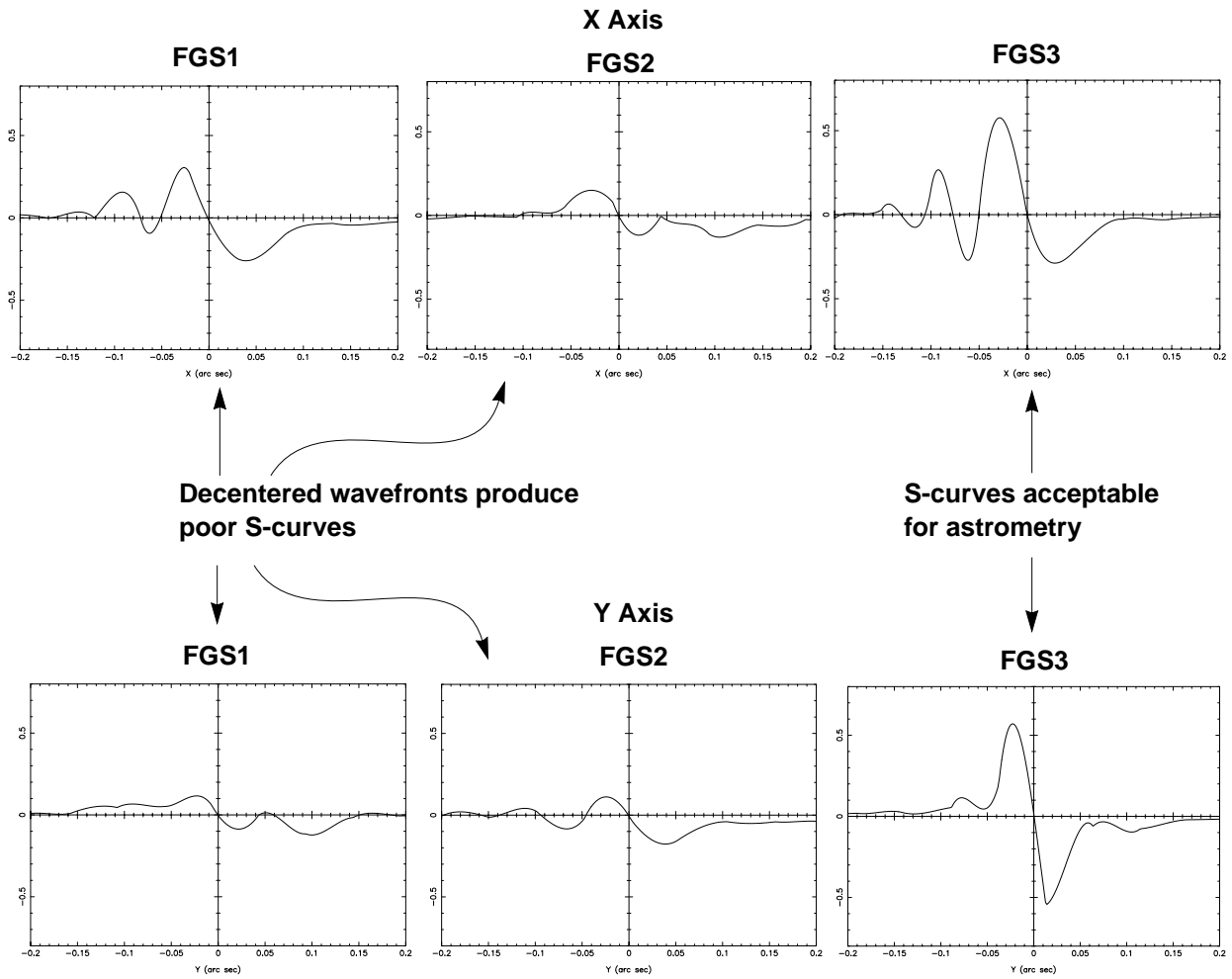
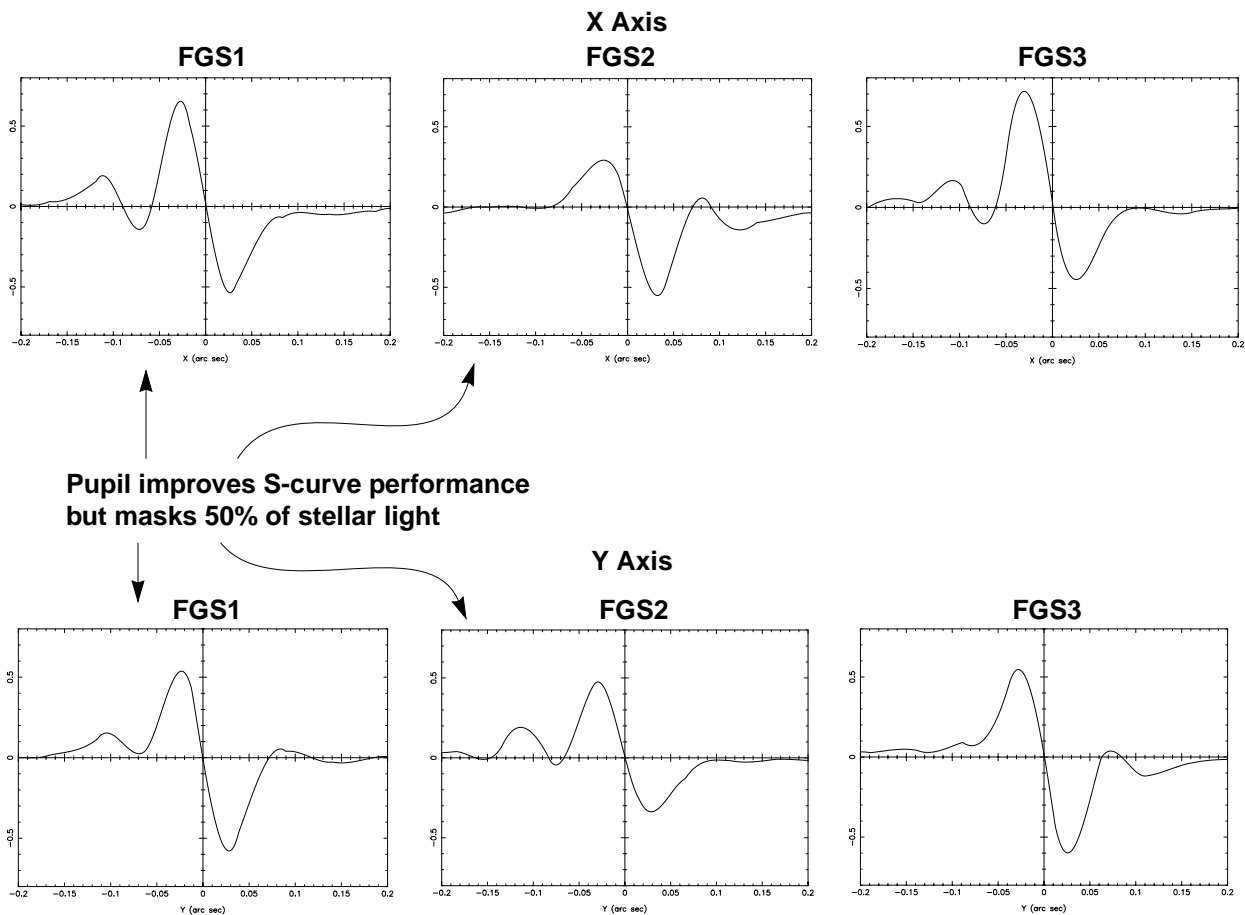


**Figure 9.8:** Dramatically Improved S-curves for FGS 1 and FGS 2 when Same Star is Observed through the 2/3 Pupil Stop



## 9.2.4 FGS 1R

The on-orbit evaluations of the FGSs in the presence of spherical aberration from the OTA has shown that proper alignment of the FGS's internal optics is absolutely essential to its performance. Moreover, the apparent decenters of the beams on the faces of the Koesters prisms for the 3 FGSs indicate that the pre-launch alignments within an FGS are not preserved once the instrument arrives in orbit. Therefore, Hughes Danbury Optical Systems, the manufacturer of the FGS, proposed that a refurbished FGS would greatly benefit from a commandable adjustment mechanism that recenters the beam at the Koesters prism. The replacement FGS in radial bay #1, installed on HST during the 1997 servicing mission and referred to as FGS 1R has such a mechanism. In essence one of the static plane fold flat mirrors (FF3) was replaced with an articulating mirror which can be commanded to place the output beam from the Star Selector B assembly at the centers of the two Koesters prisms. Unfortunately, this correction does not fix field dependency because any beam walk from SSB at the

Koesters prism will remain. The FF3 mechanism can center the beam for only one SSB rotation angle.

The FF3 has been adjusted to yield near perfect S-curve performance at the center of FGS 1R's pickle. And although the S-curves of FGS 1R show field dependency, it is not as extreme as that in FGS 3. Therefore, with excellent S-curves at pickle center and improved performance (relative to FGS 3) everywhere else, FGS 1R is potentially the best astrometric science instrument onboard HST. Figure 9.9 and Figure 9.10 compare the S-curves from three positions in the pickle of FGS 3 with those from FGS 1R.

**Figure 9.9:** Field Dependency of FGS3 Across the Pickle

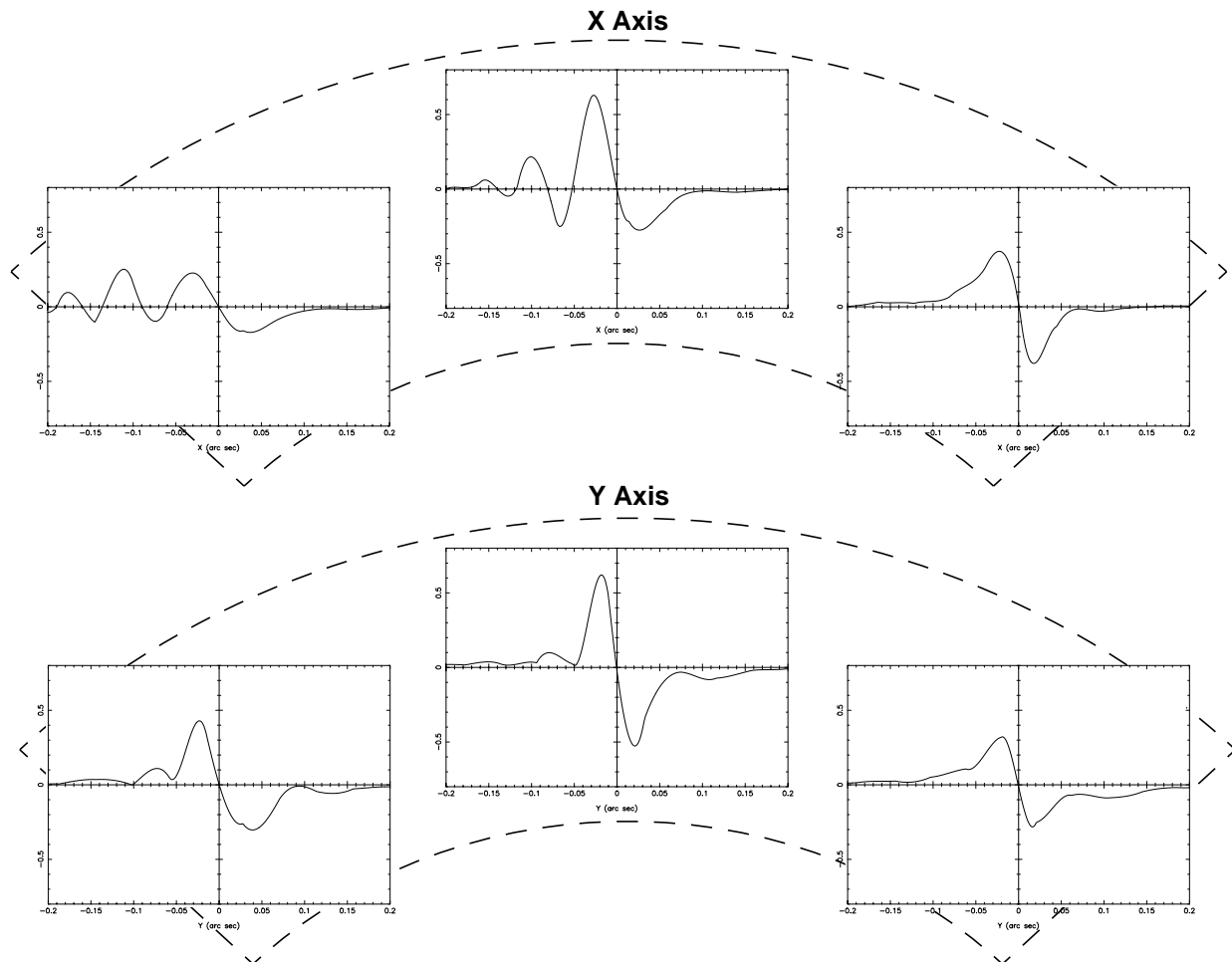
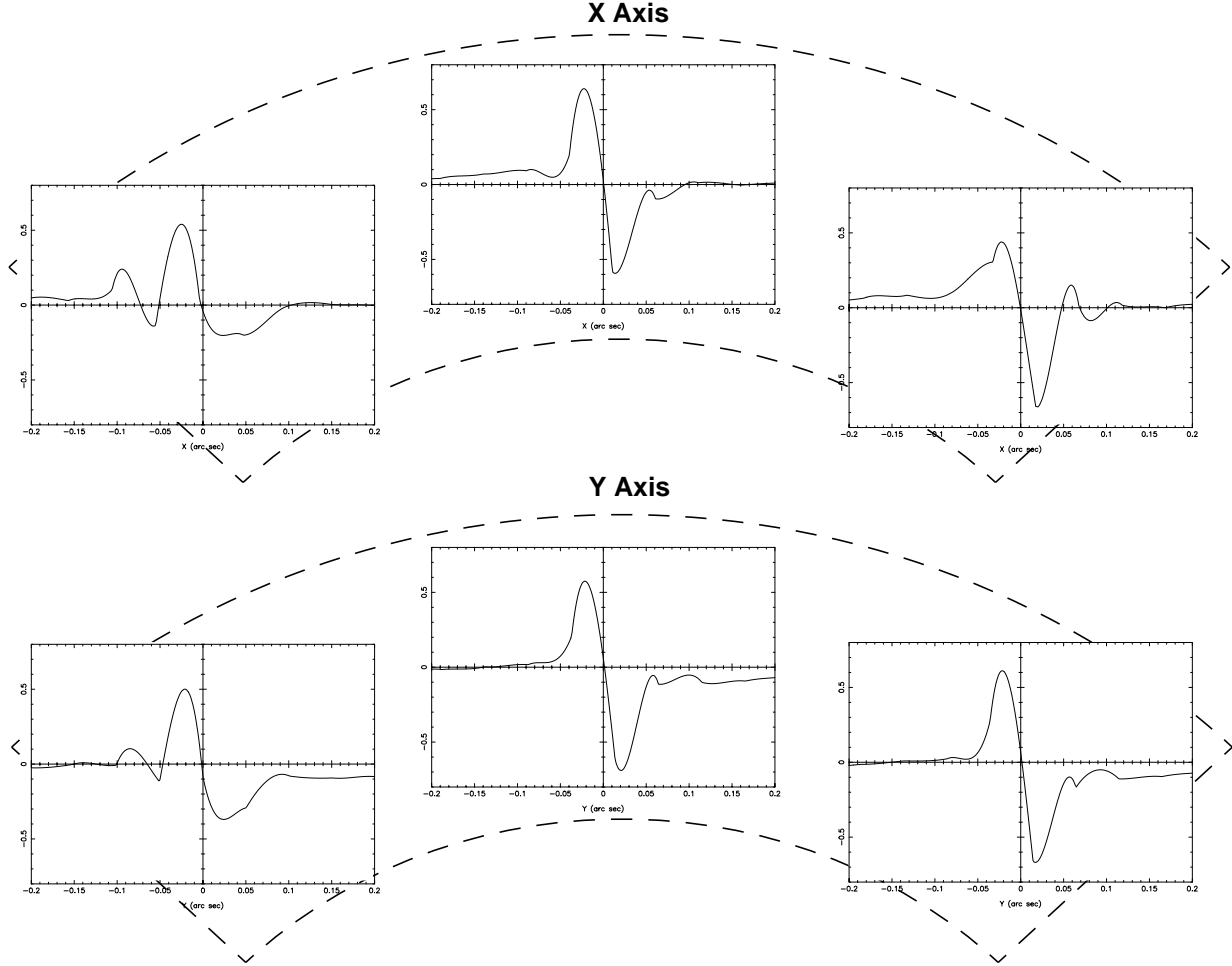


Figure 9.10: Field Dependency of FGS1R Across the Pickle



FGS/9

### 9.3 FGS Control

Two different kinds of computers can control the three FGSs. One is HST’s housekeeping computer, the DF 224. The other is the Fine Guidance Electronics (FGE) microprocessor associated with each FGS. Both the FGEs and the DF 224 control the FGSs while they are guiding HST. However, when one of the FGSs is being used as an astrometer in POSITION mode, its FGE controls it, and when it is scanning in TRANSFER more, the DF 244 controls it.

The fundamental time interval for an FGS is 25 milliseconds, the shortest time over which the FGSs can compute a fine error signal or respond to commands. Independent of instrument mode or activity, the DF 224 gathers all FGS data at 25 millisecond intervals, assigns them specific locations in the engineering telemetry stream, and downlinks them to the ground. The engineering telemetry format at

the time of transmission determines what FGS data are included in the downlink and the rates at which they are reported.

---

## 9.4 Target Acquisition and Tracking

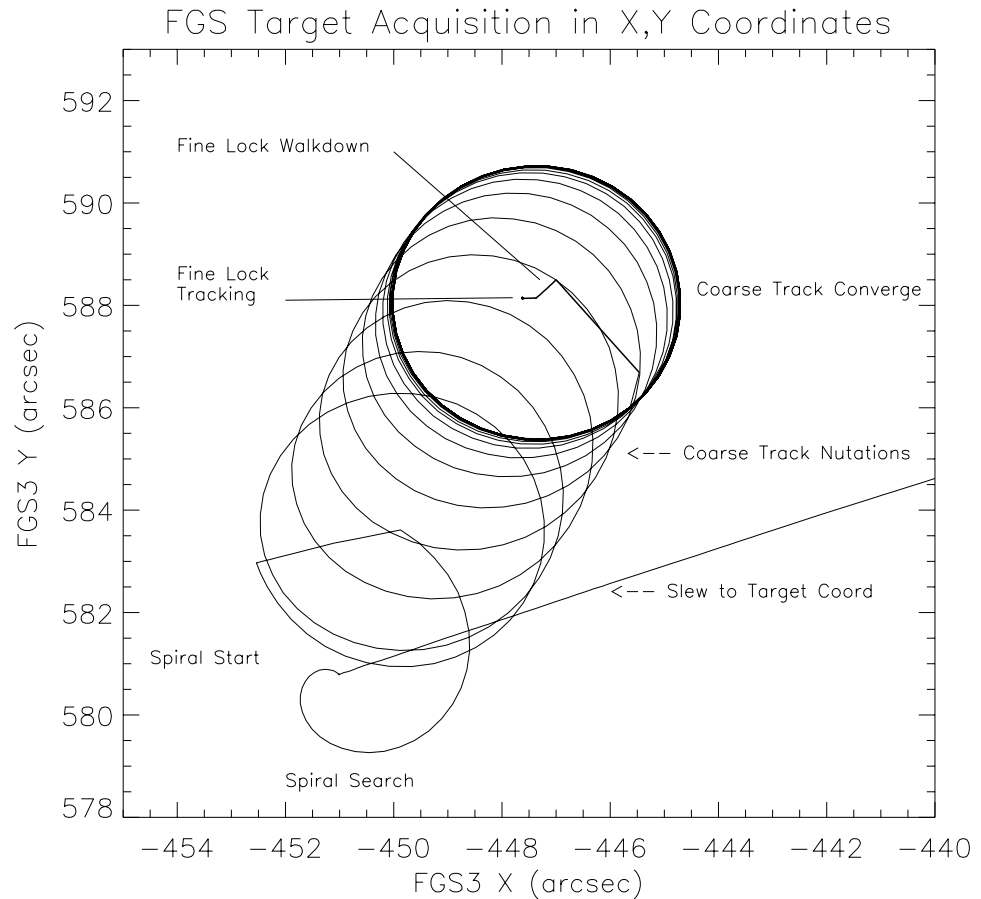
An FGS astrometry dataset contains all the steps in the target acquisition and tracking sequence. This information is necessary because the calibration pipeline uses it in the data reduction process. In this section we describe the acquisition and tracking sequence and define the flags and status bits that record the activities during the acquisition.

The first step in using an FGS either as a guider or an astrometer is to acquire the target in its instantaneous field of view. To accomplish this task, the DF 224 slews the FGS's IFOV to the expected position of the target within its pickle. (Uplinked commands specify the SSA and SSB rotation angles that should put the IFOV on the star.) Once the IFOV arrives at the expected position of the star, the DF 224 delegates control of the FGS to its FGE, which attempts to locate and to track the star by implementing its Search, CoarseTrack, and FineLock algorithms.

Figure 9.11 illustrates the movement of the IFOV during a target acquisition, showing:

1. The end of the slew to the target's expected location.
2. A short spiral search.
3. Coarse track nutations to locate the photocenter.
4. WalkDown to locate interferometric null.
5. Tracking of the star in FineLock.

This particular case was chosen for its clear demonstration of the phases of the acquisition. It is, however, atypical because the 7" difference between the expected location and the true location of the target is unusually large.

**Figure 9.11:** Location of IFOV as FGS Acquires a Target

### 9.4.1 Search

The IFOV, under FGE control, steps every 25 msec along an outward spiral while the PMTs count the photons received from the 5" x 5" patch of sky in the IFOV over the same 25 msec. When the counts fall within a specified range, the FGE declares the spiral search a success, and the instrument proceeds to the next phase of the acquisition, CoarseTrack. Otherwise, the FGE continues the spiral search until it either finds the star or completes its maximum search radius, typically 15" for astrometry and 90" for guiding. If no star is detected, the attempt is classified a failure, and the FGE halts further activity.

### 9.4.2 CoarseTrack

Having successfully completed its SEARCH, the FGE then attempts to acquire and track the star in CoarseTrack. In this mode the FGS determines the photocenter of light by comparing the photon counts from the 4 PMTs as the IFOV nutates in a 5" diameter circular path around the target. Data from each

nutations are used to verify that the star is still in view and to adjust the path of the next nutation to improve the centering of the star. If the FGS is being operated as an astrometer in POSITION mode, the FGE will initiate the FineLock acquisition after a specified number of nutations: 13 for bright,  $mv < 14$  objects, 21 for fainter objects. If the FGS is being operated as a guider or as an astrometer in TRANSFER mode, it remains in CoarseTrack until instructed by the DF 224 to initiate an attempt at FineLock.

If the PMT data ever indicate that the star is no longer present, the FGS reverts back to SEARCH mode, beginning where it left off on the search spiral to resume its outward search for the star.

### 9.4.3 FineLock

Upon completion of the CoarseTrack, either autonomously or by order of the DF 224, the FGE assumes control of the FGS and attempts to acquire the target in FineLock. This activity involves two distinct phases, acquisition and tracking. Both make use of the interferometric signal (the S-curve) to achieve success. The fundamental interval of time during FineLock is the *fine error averaging time* denoted as FESTIME. During an FESTIME the FGS integrates the PMT data while holding the IFOV fixed.

This acquisition phase is called “WalkDown to FineLock,” or simply *the WalkDown*. The FGE commands the FGS’s IFOV to a position offset or “backed-off” from the photocenter (determined by CoarseTrack). The back-off distance, equal in (+dx,+dy), is specified by the uplinked command parameter *KB*:

$$KB = \sqrt{dx^2 + dy^2}$$

For FGS 3 POSITION mode astrometry observations, *KB* is set to 0.3”. For TRANSFER mode observations, *KB* is half the scan length plus an adjustment to compensate for a known bias in the CoarseTrack to FineLock centroids (the difference between the photocenter location and interferometric null).

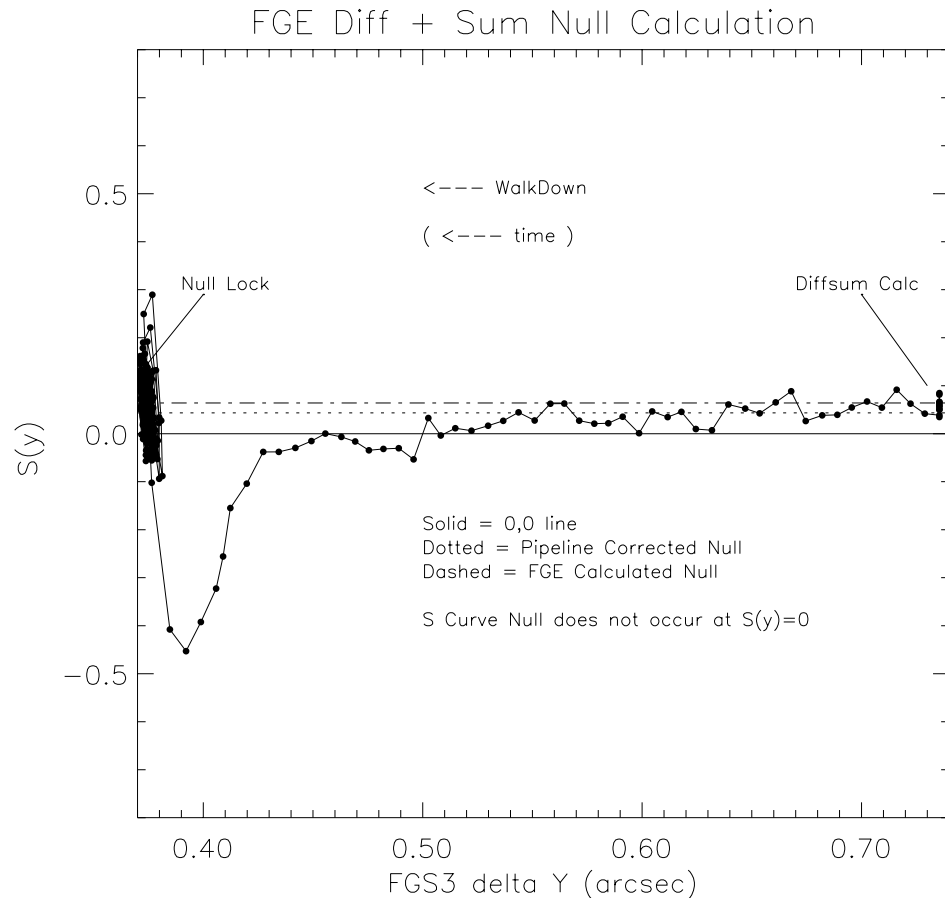
Once the IFOV arrives at the starting point, its position is held fixed for 0.4 SECONDS or an FESTIME, whichever is longer. The FGE collects data from the 2 PMTs on each of the x and y channels to compute an average sum (SUM) and difference (DIFF) on each channel. The DIFF and SUM values compensate for any difference in the response of the two PMTs on a given axis. Thus, the x-axis fine error signal (FES) for the remainder of a POSITION mode observation will be:

$$Q_x = (A_x - B_x - DIFF_x) / SUM_x$$

where  $A_x$  and  $B_x$  are the average photon counts/25msec (from PMTXA and PMTXB) integrated over the FESTIME, and  $DIFF_x$  and  $SUM_x$  are the average difference and sum of the PMTXA, PMTXB counts/25msec (determined while the IFOV was held fixed at the starting point of the WALKDOWN). The y-axis FES is computed in a similar fashion. Figure 9.12 shows the instantaneous value of the normalized difference of the PMT counts along the y-axis during a Walk-

Down to FineLock. The fact that the null lies to the positive side of  $S_y = 0.0$  clearly demonstrates the need for the DIFF-SUM adjustment to locate the true interferometric null (where  $Q_y = 0$ ).

**Figure 9.12:** Offset of True Null from  $S_y = 0$



During the WalkDown the IFOV creeps towards the photocenter in a series of equal steps, approximately  $0.006''$  in  $x$  and  $y$ , and is held fixed for an FESTIME while the PMT data are integrated to compute the fine error signal on each axis. If the absolute value of the fine error signal for a given axis exceeds a command specified threshold for three consecutive steps, satisfying the *3-hit algorithm*, the FGE concludes that it has encountered the S-curve on that axis. From this point on, a continuous feedback loop between the star selector servos and the value of the fine error signal governs the repositioning of the IFOV along that axis from this point on. The FGS continuously adjusts the star selector positions by small rotations after every FESTIME interval to set the fine error signal to zero, repositioning the IFOV so that the wavefront presented to the face of the Koesters prism has zero tilt.

The FGS tracks the star in FineLock by keeping the IFOV loitering about the star's interferometric null (the zero-point crossing of the fine error signal). Once

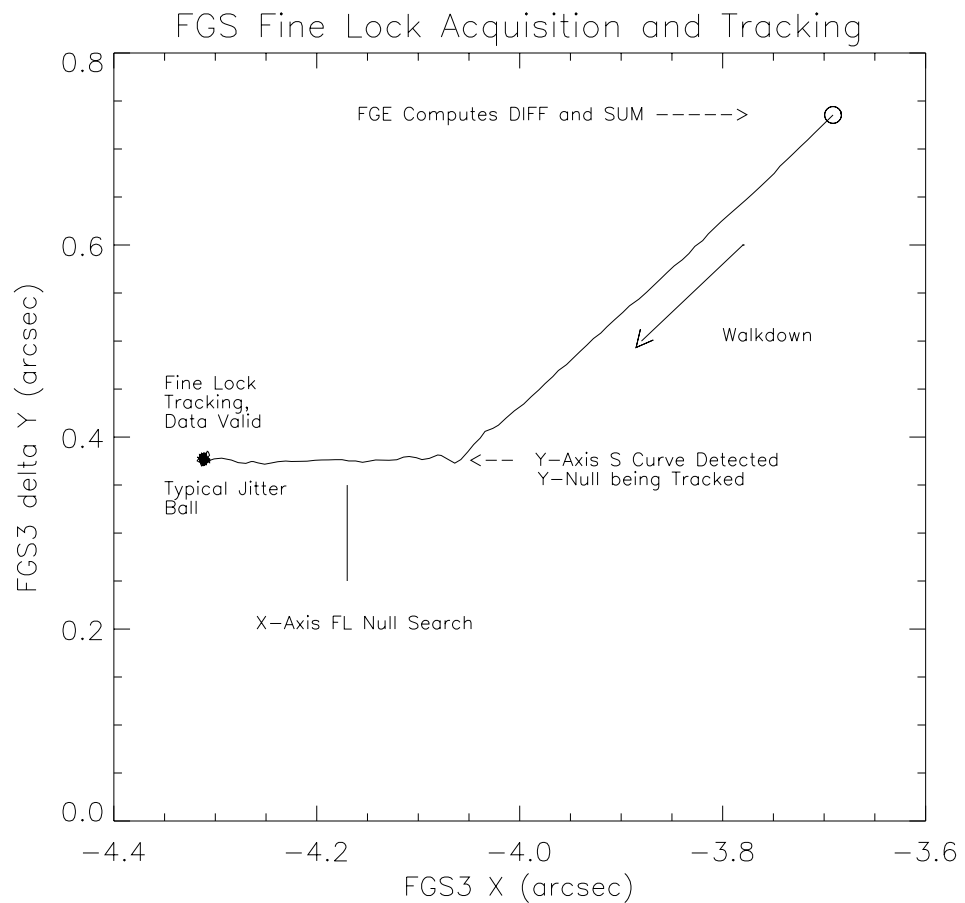
the S-curve has been encountered on, say, the  $x$ -axis, the correction to the current position of the IFOV along the  $x$ -axis for the next FESTIME is computed by

$$dx = KI_x * Q_x + KO_x$$

where  $KI_x$  and  $KO_x$  are uplinked command parameters called K-factors.

When the S-curves on both axes have been encountered and have satisfied the 3-hit algorithm, the FGS is said to be tracking the object in FineLock and the FGE sets the DataValid status flag. Figure 9.13 shows the IFOV for both the WalkDown and FineLock tracking in local detector space. Notice that interferometric null is located first along the  $y$ -axis, and the IFOV must walk an additional 0.2" along the  $x$ -axis to find the  $x$ -axis null. This is typical of FGS 3 and is due to the effect of field stop misalignments on the Coarse Track measurements

**Figure 9.13:** X,Y Position in Detector Space of FGS 3's IFOV During Walkdown to FineLock and Subsequent Tracking of a Star in FineLock



---

## 9.5 Transfer Scans

The acquisition of an object for an FGS operating in TRANSFER mode is carried out in the same sequence described above, with the exception that the FGS remains in CoarseTrack until a specified spacecraft time. Thereafter it proceeds to FineLock by slewing the IFOV to the starting point of the first scan. As described earlier for the POSITION mode WalkDown, the FGS averages and differences the PMT data for 0.4 seconds, computes the fine error signal, and compares it to a commanded threshold. However, this threshold equals zero for TRANSFER mode observations, immediately prompting the FGE to declare that FineLock has been achieved and to set the DataValid flag. Setting this flag signals the DF 224 that the FGS is ready to begin the TRANSFER mode observation.

In a TRANSFER mode observation the DF 224 computer steps the FGS's IFOV across the photocenter (determined by CoarseTrack) along a diagonal path in detector space for a distance specified in the original proposal. Each sweep across the target is referred to as a scan. After the completion of a given scan, the IFOV reverses direction and scans the object again until the total number of scans specified in the proposal have been completed. Every 25 msec the PMT data and star selector rotation angles are reported in the telemetry. The FGS samples the entire S-curve, which can be reconstructed by post observation data processing.

---

## 9.6 FGS Guiding

When an FGS is used for guiding HST, it acquires a *guide star* in FineLock. The HST pointing control system then corrects telescope's pointing to bring this guide star (by slewing the telescope) to a pre-determined  $(x,y)$  position within the pickle of the guiding FGS. Once HST is properly pointed, the FGS continues to track its target in FineLock under control of both the FGE and the DF 224 while the pointing control system monitors the  $(x,y)$  position of the guide star and averages that data to determine the current pointing of the telescope. The pointing control system uses these data to eliminate translational and rotational drift of the observatory and to repoint the telescope properly. It also compensates for differential velocity aberration, which is the field-dependent change in the apparent positions of stars owing to the telescope's motion transverse to the direction it is pointed. Because pointing requires two dimensional control, two FGSs are usually used simultaneously to track guide stars. The FGS that controls translational attitude is the *dominant guider*, and the FGS that controls roll is the *roll* or *subdominant guider*.

Sometimes only one FGS actively guides the telescope, maintaining only translational control. Then HST is "free" to roll about the dominant guide star, restrained only by gyroscopic feedback. This situation arises more frequently during astrometry observations than for the other observations because guide star candidates, which can be difficult to find in the first place, are limited to those which appear in two FGSs instead of three.

The FGS astrometry pipeline uses data from the guiding FGSs to provide a high-resolution spatial and temporal HST pointing history over the course of an astrometry observation. These guide star data are useful in both POSITION mode and TRANSFER mode data reductions.

---

## 9.7 FGS Astrometry

The two astrometry modes of the FGS are POSITION mode and TRANSFER mode. An FGS in POSITION mode acquires an object in FineLock and tracks it for an extended period of time. An FGS in TRANSFER mode acquires an object and scans the IFOV back and forth along a 45° diagonal path in detector space to sample the interference pattern fully enough to construct an S-curve.

### POSITION Mode Observing

POSITION mode observing with the FGS can determine the parallax, proper motion, and/or reflex motion of a given object. A typical POSITION mode observing program, regardless of the scientific goal, measures the (x,y) detector space positions of several objects concurrently observable in FGS's total FOV, or pickle. An FGS can observe only one object at a time, so each of the objects are visited and tracked in FineLock in a sequence specified by the proposal. The DF 224 slews the IFOV of the astrometer to the expected location of the first star in the sequence and relinquishes control to the FGE. The FGE then commands the FGS to acquire and track the target via the Search, CoarseTrack, and FIneLock sequences. Later, at a specific spacecraft clock time, the DF 224 resumes control of the FGS, terminates the FineLock tracking of the object and slews the IFOV to the expected location of the next star in the sequence. This process repeats until the FGS has observed all stars in the observation set belonging to that visit. (The time an FGS tracks a given object in FineLock is usually some 20 seconds longer than the exposure time specified in the proposal because of unused overheads.)

### TRANSFER Mode Observing

TRANSFER mode observing with the FGS can resolve the components of multi-star systems and measure the angular dimensions of extended objects. In a TRANSFER mode observation the FGS acquires the object as described above, but instead of attempting to keep the FGS's IFOV at or near interferometric null as in a POSITION observation, the FGS, under control of the DF 224, steps its IFOV is back and forth across the object along a 45 deg diagonal path in detector space, sampling the entire S-curve and its immediate vicinity. Each sweep across the object is referred to as a *scan*. The number of scans, size of each step, and length of each scan are specified in the proposal. Typically, a TRANSFER mode observation will consist of 20 or more scans, each 1.4" long, with a step size of 1 mas.

### Mixed Mode Observing

It is sometimes possible to determine the parallax, proper motion, and reflex motion of a multiple star system resolvable by the FGS in TRANSFER mode. If the FGS can both resolve a binary system and measure its parallax, then the

absolute masses of its components would be determined. To accomplish such tasks, the FGS observes the target in TRANSFER mode and other nearby stars in POSITION mode. A mixed mode observing strategy would include a series of POSITION mode observations of the reference stars and a TRANSFER mode observation embedded somewhere in the sequence. Although the post-observation analysis of mixed mode observing data can be challenging, the potential scientific returns have made it an increasingly popular way to use the FGS as an astrometer.

---

## 9.8 Astrometry with FGS 3

Among the three FGSs on HST, only FGS 3 has been calibrated and used as an astrometer because the performance of FGS 1 and FGS 2 is not adequate for astrometric science (see “S-curves” on page 9-8). This section will discuss the overall performance characteristics of FGS 3 in both POSITION mode and TRANSFER mode.

### POSITION Mode Characteristics

When FGS 3 is used as an astrometer, the “full” F583W wide bandpass spectral filter is used in POSITION mode for stars of  $V > 8$  to maximize the sensitivity. The F5ND attenuator is used for stars with  $V < 8$ . The instrumental properties affecting POSITION mode observation planning and data calibration are: the spatial dependence of the S-curve, the optical field angle distortions across the pickle, and the slow temporal changes in the plate scale, probably due to outgassing of the graphite epoxy. In those areas of the pickle with lower S/N in the S-curve, the limiting magnitude rises from  $V = 17$  to  $V = 15$ . A large area in the central region of the pickle has adequate signal to noise so this problem affects observations only at the edges.

The calibration of optical field angle distortion (OFAD; see “Processing Individual Observations” on page 11-4) involves a fifth-order two-dimensional polynomial fit to observations of an astrometric standard field. The measured coordinates of a target are corrected in the pipeline using the transformation defined by these polynomial coefficients. The temporal changes to the plate scale and the OFAD are monitored on a monthly or bi-monthly basis via observations of a standard astrometric field and are provided as updates to the calibration database. In spite of the field dependent behavior of FGS 3, the repeatability and hence the accuracy of individual POSITION mode measurements of stars distributed throughout the pickle is typically about 1.5 mas for  $V < 14.5$  and about 2 mas for fainter objects. These numbers are determined from the residuals of plate overlays in which the pickle’s orientation on the sky is constant from plate to plate, so that field-dependent (OFAD) corrections do not enter. However, when the OFAD correction is required, the overall pickle-wide error budget increases to about 2.7 mas.

### TRANSFER Mode Characteristics

The S-curves of FGS 3 display strong field dependency on both the  $x$  and  $y$  axis. Each of these S-curves is nearly ideal at one location in the pickle, but the

optimal position for the  $x$  axis does not coincide with that for the  $y$  axis. This lack of coincidence has affected the astrometric performance of FGS 3 because science observations in TRANSFER mode are executed at only one position, pickle center. Any other position could be used, but pickle center was chosen as an optimal compromise and is the only position in FGS 3 supported by the TRANSFER mode calibration database. The  $y$ -axis sports a nearly ideal S-curve, while that on the  $x$ -axis suffers from aberrations.

Because the  $x$ -axis has the degraded S-curve, it is the limiting factor in the TRANSFER mode performance of FGS 3. When the projected angular separation of a binary system along the  $x$ -axis is less than about 20 mas, it is not resolved on the  $x$ -axis. On the other hand, the  $y$ -axis has been shown to resolve systems with separations as small as 10 mas. (The success at resolving the individual components depends, of course, on the magnitude difference: the larger the delta magnitude, the more difficult the observation.) This suggests that FGS 1R, with its nearly ideal S-curves on both axis at the same place in the pickle (at the center), should be able to resolve binary systems with separations on the order of 10 mas, and perhaps to detect structure in an object at the 5 mas level.